Annual Report 2022

Jaan Einasto
and Tartu Observatory cosmology group

1 Research

In this Section the work is described I made together with my collaborates. The work is described using Abstracts of papers and is divided into sections.

Astronomical data show that universe is filled with mysterious dark matter and dark energy, and that ordinary matter with stars, galaxies and interstellar gas form only about 5 per cent of the mass budget. Theoretical considerations suggest that dark matter forms the skeleton of the universe, and visible matter is located only at tips of the dark matter landscape like snow in high mountains. The difference in the distribution of galaxies and dark matter is seen in the picture below, where the left panel shows the distribution of dark matter in a slice of the simulated universe, and the right panel the distribution of simulated galaxies in the same region. In the left panel we see numerous low-density filaments, absent in the distribution of galaxies, where visible galaxies occupy only high-density peaks, which form a few per cent of the total volume of the space (pictures are based on numerical simulation on the evolution of the cosmic web, done in Tartu Observatory). Astronomers call this phenomenon 'biasing' - galaxies are biased tracers of the underlying dark matter. To measure the biasing effect quantitatively a bias parameter is used, which is equal to unity when galaxies trace mass, and is larger than unity when galaxies trace only high-density regions of matter. Here several questions arise: What is the value of bias parameter now and how it evolved with time?

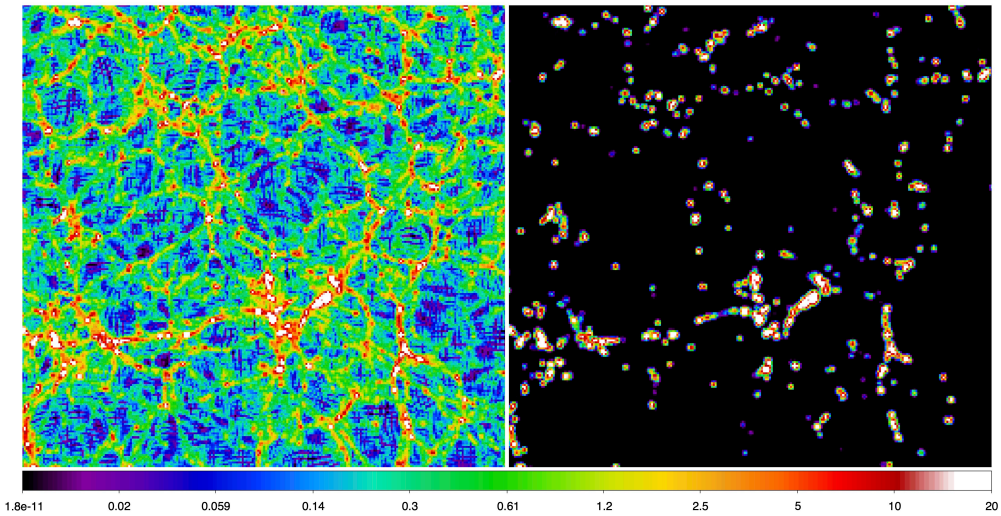

Jaan Einasto, Lauri-Juhan Liivamägi and Maret Einasto from Tartu Observatory published a study titled "The time evolution of bias" in Monthly Notices of the Royal Astronomical Society (Einasto et al., 2023). To investigate the evolution of bias parameter with cosmic epoch authors used numerical simulations of the evolution of cosmic web. Authors calculated the time evolution of the bias parameter, starting from an early epoch where the universe was only several millions years old, to the present epoch where the universe is 13.8 billion years old. The study shows that during the evolution the bias parameter decreases. The basic result of the study indicates that the bias parameter depends on two factors: the higher is the fraction of matter in voids and the higher is the luminosity of galaxies, the larger is the bias parameter.

The first evolutionary trend can be explained by the flow of matter from voids to galaxies. However, gravity cannot deplete voids completely, thus there is always some unclustered matter in voids, and the bias parameter of galaxies is always greater than unity, over the whole range of evolution epochs. Earlier investigations suggested that galaxies trace matter. The present study shows that the early belief explains only the dependence of the bias parameter on the luminosity of galaxies, but its dependence on void factor was not taken into account.

2 Conferences and popular talks

In May 3 — 6 Tuorla-Tartu Cosmology Meeting 2022 "Interaction of the cosmic matter" took place with most members of Tartu cosmology group.

In May 23 – 27 I participated in a seminar in Paris Observatory and had discussions with French astronomers. Maret Einasto had a talk in Paris Observatory seminar.

In October 24 – 31 I participated in the celebration of Nobel Price of Prof. James Peebles in Princeton University. I had a talk on the evolution of bias in Neta Bahcall lunch seminar on October 25 (Einasto et al., 2023).

3 Scientific organisations, awards

I am member of the International Astronomical Union (1961), Estonian Academy of Sciences (1981), American Astronomical Society (1981), European Astronomical Society (1990), Academia Europaea (1990), Royal Astronomical Society (1994).

I have Estonian Science Prizes (1982, 1998, 2003, 2007), Gauss Professor of the Göttingen University (1993), The Estonian Order of the National Coat of Arms (1998), Marcel Grossmann Award (2009), honorary Doctor of Tartu University (2010), Viktor Ambartsumian International Prize (2012), Doctor Honoris Causa degree of the Turku University (2013), Gruber International Cosmology Award (2014), Estonian Academy of Sciences Harald Keres medal (2019), Tartu University great medal (2019)..

4 Research – Tartu Observatory cosmology group

In this Section the work is described done in Tartu Observatory cosmology group, in addition to the work described in Section 1. This overview is based on abstracts written by authors of respective papers.

4.1 Collection of new data

Laur et al. (2022): Context. The importance of photometric galaxy redshift estimation is rapidly increasing with the development of specialised powerful observational facilities. Aims: We develop a new photometric redshift estimation workflow TOPz to provide reliable and efficient redshift estimations for the upcoming large-scale survey J-PAS which will observe 8500 deg2 of the northern sky through 54 narrow-band filters. Methods: TOPz relies on template-based photo-z estimation with some added J-PAS specific features and possibilities. We present TOPz performance on data from the miniJPAS survey, a precursor to the J-PAS survey with an identical filter system. First, we generated spectral templates based on the miniJPAS sources using the synthetic galaxy spectrum generation software CIGALE. Then we applied corrections to the input photometry by minimising systematic offsets from the template flux in each filter. To

assess the accuracy of the redshift estimation, we used spectroscopic redshifts from the DEEP2, DEEP3, and SDSS surveys, available for 1989 miniJPAS galaxies with $r < 22$ magAB. We also tested how the choice and number of input templates, photo-z priors, and photometric corrections affect the TOPz redshift accuracy. Results: The general performance of the combination of miniJPAS data and the TOPz workflow fulfills the expectations for J-PAS redshift accuracy. Similarly to previous estimates, we find that 38.6% of galaxies with $r < 22$ mag reach the J-PAS redshift accuracy goal of $dz/(1+z) < 0.003$. Limiting the number of spectra in the template set improves the redshift accuracy up to 5%, especially for fainter, noise-dominated sources. Further improvements will be possible once the actual J-PAS data become available.

de Jong et al. (2022): 4MOST is a new high-multiplex, wide-field spectroscopic survey facility under construction for ESO's 4m-VISTA telescope at Paranal, Chile. Its key specifications are: a large field of view of 4.4 square degrees, a high multiplex fibre positioner based on the tilting spine principle that positions 2436 science fibres in the focal surface of which 1624 fibres go to two low-resolution optical spectrographs ($R = \lambda/\Delta\lambda$ 6500) and 812 fibres transfer light to the high-resolution optical spectrograph ($R \sim 20,000$). Currently, almost all subsystems are completed and full testing in Europe will be finished in spring 2023, after which 4MOST will be shipped to Chile. An overview is given of instrument construction and capabilities, the planned science of the consortium and the recently selected community programmes, and the unique operational scheme of 4MOST.

4.2 Cosmic web: structure of superclusters

Einasto et al. (2022a) studied the evolution of galaxies which is influenced by their local and global environment in the cosmic web. Galaxies with very old stellar populations (VO galaxies with Dn(4000) index ≥ 1.75) mostly lie in the centres of galaxy clusters, where they evolve under the influence of processes characteristic of high-density cluster environments. However, VO galaxies have also been found in poor groups in global low-density environments between superclusters, which we call watershed regions. Aims: Our aim is to analyse the properties of galaxies in various cosmic environments with a focus on VO galaxies in the watershed regions to understand their evolution, and the origin of the large-scale morphology-density relation. Methods: We employ the Sloan Digital Sky Survey DR10 MAIN spectroscopic galaxy sample in the redshift range $0.009 \leq z \leq 0.200$ to calculate the luminosity-density field of galaxies, to determine groups and filaments in the galaxy distribution, and to obtain data on galaxy properties. The luminosity-density field with smoothing length 8 h^{-1} Mpc, D8, characterises the global environment of galaxies. We analyse the group and galaxy contents of regions with various D8 thresholds. We divide groups into low- and high-luminosity groups based on the highest luminosity of groups in the watershed region, $L_{gr} \leq 15 \times 10^{12}\ h^{-2} L_{\odot}$. We compare the stellar masses, the concentration index, and the stellar velocity dispersions of quenched and star-forming galaxies among single galaxies, satellite galaxies, and the brightest group galaxies (BGGs) in various environments. Results: We show that the global density is most strongly related to the richness of galaxy groups. Its influence on the overall star formation quenching in galaxies is less strong. Correlations between the morphological properties of galaxies and the global density field are the weakest. The watershed regions with $D8 < 1$ are populated mostly by single galaxies, constituting 70% of all galaxies there, and by low-luminosity groups. Still, approximately one-third of all galaxies in the watershed regions are VO galaxies. They have lower stellar masses, smaller stellar velocity dispersions, and stellar populations that are up to 2 Gyr younger than those of VO galaxies in other global environments. In higher density global environments ($D8 > 1$), the morphological properties of galaxies are very similar. Differences in galaxy properties are the largest between satellites and BGGs in groups. Conclusions: Our

results suggest that galaxy evolution is determined by the birthplace of galaxies in the cosmic web, and mainly by internal processes which lead to the present-day properties of galaxies. This may explain the similarity of (VO) galaxies in extremely different environments.

Heinämäki et al. (2022) studied superclusters as systems with varied properties and varied fractional overdensities. Their dynamical state evolves under the influence of two components: dark energy and gravitational force. The dominant component at any spatial location and cosmic epoch is determined by the total mass and the local overdensity of the system. However, generally the dynamical state of superclusters is poorly known. Aims: We study properties of superclusters and select a sample of quasi-spherical superclusters, the dynamics of which can be studied using the Λ significance diagram. Methods: We extracted our supercluster sample with an adaptive local threshold density method from the Sloan Digital Sky Survey Data Release 7 (SDSS DR7) data and estimated their masses using the dynamical masses for member galaxies and groups. We used topological analysis based on Minkowski functionals and the positions of galaxies and galaxy groups in superclusters. Finally, we highlight the dynamical state of a few exceptional types of superclusters found in this study using the Λ significance diagram. Results: Our final sample contains 65 superclusters in the distance range of $130-450\ h^{-1}$ Mpc. Supercluster masses range between $1.1 \times 10^{15}\ M_{\odot}$ and $1.4 \times 10^{16}\ M_{\odot}$ and sizes between 25 h^{-1} Mpc and 87 h^{-1} Mpc. We find that pancake-type superclusters form the low-luminosity, small, poor and low-mass end of superclusters. We find four superclusters of unusual types, exhibiting exceptionally spherical shapes. These so-called quasi-spherical systems contain a high-density core surrounded by a relatively spherical density and galaxy distribution. The mass-to-light ratio of these quasi-spherical is higher than those of the other superclusters, suggesting a relatively high dark matter content. Using the Λ significance diagram for oblate and prolate spheroids, we find that three quasi-spherical superclusters are gravitationally bound at the present epoch. Conclusions: Quasi-spherical superclusters are among the largest gravitationally bound systems found to date, and form a special class of giant systems that, dynamically, are in between large gravitationally unbound superclusters and clusters of galaxies in an equilibrium configuration.

Einasto et al. (2022b) studied high-density cores (HDCs) of galaxy superclusters, that embed rich clusters and groups of galaxies are the earliest large objects to form in the cosmic web, and the largest objects that may collapse in the present or future. Aims: We aim to study the dynamical state and possible evolution of the HDCs in the BOSS Great Wall (BGW) superclusters at redshift $z \approx 0.5$ from the CMASS (constant mass) galaxy sample, based on the Baryon Oscillation Spectroscopic Survey (BOSS) in order to understand the growth and evolution of structures in the Universe. Methods: We analysed the luminosity density distribution in the BGW superclusters to determine the HDCs in them. We derived the density contrast values for the spherical collapse model in a wide range of redshifts and used these values to study the dynamical state and possible evolution of the HDCs of the BGW superclusters. The masses of the HDCs were calculated using stellar masses of galaxies in them. We found the masses and radii of the turnaround and future collapse regions in the HDCs of the BGW superclusters and compared them with those of local superclusters. Results: We determined eight HDCs in the BGW superclusters. The masses of their turnaround regions are in the range of $MT \approx 0.4 - 3.3 \times 10^{15} h^{-1} M_{\odot}$ and radii are in the range of $RT \approx 3.5 - 7\ h^{-1}$ Mpc. The radii of their future collapse regions are in the range of $RFC \approx 4 - 8\ h^{-1}$ Mpc. Distances between individual cores in superclusters are much larger: of the order of $25 - 35 h^{-1}$ Mpc. The richness and sizes of the HDCs are comparable with those of the HDCs of the richest superclusters in the local Universe. Conclusions: The BGW superclusters will probably evolve to several poorer superclusters with masses similar to those of the local superclusters. This

may weaken the tension with the ΛCDM model, which does not predict a large number of very rich and large superclusters in our local cosmic neighbourhood, and explains why there are no superclusters as elongated as those in the BGW in the local Universe.

Superclusters are the largest objects in the Universe, and they provide a unique opportunity to study how galaxy clusters are born at the junction of the cosmic web as well as the distribution of magnetic fields and relativistic particles beyond cluster volume (Parekh et al., 2022). The field of radio astronomy is going through an exciting and important era of the Square Kilometer Array (SKA). We now have the most sensitive functional radio telescopes, such as the MeerKAT, which offers high angular resolution and sensitivity towards diffuse and faint radio sources. To study the radio environments around supercluster, we observed the (core part of) Saraswati supercluster with the MeerKAT. From our MeerKAT Observation of the Saraswati Supercluster (MOSS) project, the initial results of the pilot observations of two massive galaxy clusters, A2631 and ZwCl2341.1+0000, which are located around the dense central part of the Saraswati supercluster, were discussed. In this paper, we describe the observations and data analysis details, including direction-dependent calibration. In particular, we focus on the ZwCl2341.1+0000 galaxy cluster, which hosts double radio relics and puzzling diffuse radio source in the filamentary network. We have imaged these double radio relics in our high resolution and sensitive L-band MeerKAT observation and a puzzling radio source, located between relics, in the low-resolution image. We also derived the spectra of double radio relics using MeerKAT and archival GMRT observations. The following papers will focus on the formation of radio relics and halo, as well as radio galaxy properties in a supercluster core environment.

4.3 Early Universe

Hütsi et al. (2022): The James Webb Space Telescope has detected surprisingly luminous early galaxies that indicate a tension with the ΛCDM. Motivated by scenarios including axion miniclusters or primordial black holes, we consider power-law modifications of the matter power spectrum. We show that the tension could be resolved if dark matter consists of $2 \times 10 - 18$eV axions or if a fraction $fPBH > 0.005$ of dark matter is composed of compact heavy $4 \times 10^6 M_\odot$(fPBH/0.005)-1 structures such as primordial black hole clusters. However, in both cases, the star formation efficiency needs to be significantly enhanced.

4.4 Structure of clusters of galaxies

Bazarov et al. (2022): The abundance of dark matter subhalos orbiting a host galaxy is a generic prediction of the cosmological framework, and is a promising way to constrain the nature of dark matter. In this paper, we investigate the use of machine learning-based tools to quantify the magnitude of phase-space perturbations caused by the passage of dark matter subhalos. A simple binary classifier and an anomaly detection model are proposed to estimate if stars or star particles close to dark matter subhalos are statistically detectable in simulations. The simulated datasets are three Milky Way-like galaxies and nine synthetic Gaia DR2 surveys derived from these. Firstly, we find that the anomaly detection algorithm, trained on a simulated galaxy with full 6D kinematic observables and applied on another galaxy, is nontrivially sensitive to the dark matter subhalo population. On the other hand, the classification-based approach is not sufficiently sensitive due to the extremely low statistics of signal stars for supervised training. Finally, the sensitivity of both algorithms in the Gaia-like surveys is negligible. The enormous size of the Gaia dataset motivates the further development of scalable and accurate data analysis methods that could be used to select potential regions of interest for dark matter

searches to ultimately constrain the Milky Way's subhalo mass function, as well as simulations where to study the sensitivity of such methods under different signal hypotheses.

4.5 Cosmic web: missing baryons

Holt et al. (2022) present an updated scaling relation between the optical luminosity density (LD) of galaxies in the r band and the density of the warm-hot intergalactic medium (WHIM) in cosmic filaments, using the high-resolution EAGLE simulations. We find a strong degree of correlation between the WHIM density and the galaxy luminosity density, resulting in a scaling relation between the two quantities that permits us to predict the WHIM density of filaments with a scatter of less than 2 dex in a broad range of smoothed filament luminosity densities. In order to estimate the performance of the simulation-based calibration of the LD-WHIM density relation, we applied it to a sample of low-redshift filaments detected with the Bisous method in the Legacy Survey SDSS DR12 data. In the volume covered by the SDSS data, our relation predicts a WHIM density amounting to $31 \pm 7 \pm 12$ per cent (statistical errors followed by systematic) of cosmic baryon density. This agrees, albeit within the large uncertainties, with the current estimates of the cosmological missing baryon fraction, implying that our LD-WHIM density relation may be a useful tool in the search for the missing baryons. This method of analysis provides a new promising avenue to study the physical properties of the missing baryons, using an observable that is available for large volumes of the sky, complementary and independent from WHIM searches with absorption-line systems in the FUV or X-rays.

4.6 Structure and evolution of simulated galaxies

Damle et al. (2022): Recent observations have revealed remarkable insights into the gas reservoir in the circumgalactic medium (CGM) of galaxy haloes. In this paper, we characterize the gas in the vicinity of Milky Way and Andromeda analogues in the HESTIA (High resolution Environmental Simulations of The Immediate Area) suite of constrained Local Group (LG) simulations. The HESTIA suite comprise of a set of three high-resolution AREPO-based simulations of the LG, run using the Auriga galaxy formation model. For this paper, we focus only on the z = 0 simulation data sets and generate mock skymaps along with a power spectrum analysis to show that the distributions of ions tracing low-temperature gas (H I and Si III) are more clumpy in comparison to warmer gas tracers (O VI, O VII, and O VIII). We compare to the spectroscopic CGM observations of M31 and low-redshift galaxies. HESTIA underproduces the column densities of the M31 observations, but the simulations are consistent with the observations of low-redshift galaxies. A possible explanation for these findings is that the spectroscopic observations of M31 are contaminated by gas residing in the CGM of the Milky Way.

Khoperskov et al. (2022b): Theory suggests that mergers play an important role in shaping galactic disks and stellar haloes, which was observationally confirmed in the MW thanks to the Gaia data. In this work, aiming to probe the contribution of mergers to the in-situ stellar halo formation, we analyze six M31/MW analogues from the HESTIA suite of cosmological hydrodynamical zoom-in simulations of the Local Group. We found that all the HESTIA galaxies experience from 1 to 4 mergers with stellar mass ratios between 0.2 and 1 relative to the host at the time of the merger. These significant mergers, with a single exception, happened 7-11 Gyr ago. The overall impact of the most massive mergers in HESTIA is clearly seen as a sharp increase of the orbital eccentricity (and a corresponding decrease of the Vphi) of preexisting disc stars of the main progenitor, thus reproducing well the Splash/Plume-like feature discovered in the MW. We do find a correlation between mergers/close pericentric passages of massive

satellites and bursts of the star formation in the in-situ component. Massive mergers sharply increase the disc velocity dispersion of the in-situ stars, however, the latest significant merger often heats up the disk up to the numbers when the contribution of the previous ones is less prominent in the age-velocity dispersion relation. In the HESTIA galaxies, the in-situ halo is an important component of the inner stellar halo where its fraction is about 30-40%, while in the outer parts it typically does not exceed 5% beyond 15 kpc. The simulations suggest that this component of the stellar haloes continues to grow well after mergers conclude; however, the most significant contribution comes from stars formed recently before the merger. The orbital analysis of the HESTIA galaxies suggests that wedges in Rmax-Zmax space are mainly populated by the stars born in between significant mergers.

Khoperskov et al. (2022c): In the Milky Way, recent progress in the exploration of its assembly history is driven by the tremendous amount of high-quality data delivered by Gaia, which has revealed a number of substructures potentially linked to several ancient accretion events. In this work, aiming to explore the phase-space structure of accreted stars, we analyze six M31/MW analogues from the HESTIA suite of cosmological hydrodynamics zoom-in simulations of the Local Group. We found that all the HESTIA galaxies experience a few dozen mergers but only 1-4 mergers have the stellar mass ratio ¿0.2 where, depending on the halo definition, the most massive merger contributes from 20% to 70% of the total stellar halo. Individual merger remnants show diverse density distributions at z=0, significantly overlapping with each other and with the in-situ stars in the ELz, UV and RVphi coordinates. The mergers debris often change their position in the ELz with time due to the galactic mass growth and the non-axisymmetry of the potential. In agreement with previous works, we show that even individual merger debris exhibit a number of distinct ELz features. In the UV plane, all HESTIA galaxies reveal radially hot, non-rotating or weakly counter-rotating, Gaia-Sausage-like features. We found an age gradient in Elz space for the individual debris, where the youngest stars, formed in the inner regions of accreting systems, deposit to the innermost regions of the host. The bulk of these stars is being formed during the last stages of accretion, making it possible to date the merger. In actions space (Jr, Jz, Jϕ), the mergers debris do not appear as isolated substructures but are instead scattered over a large parameters area and overlapping with the in-situ stars. We also introduce a purely kinematic space (Jz/Jr-eccentricity), where different merger debris can be disentangled better from each other and from the in-situ stars.

Khoperskov et al. (2022a): Since the chemical abundances of stars are the fossil records of the physical conditions in galaxies, they provide the key information for recovering the assembly history of galaxies. In this work, we explore the chemo-chrono-kinematics of accreted and in-situ stars, by analyzing six M31/MW analogues from the HESTIA suite of cosmological hydrodynamics zoom-in simulations of the Local Group. We found that the merger debris are chemically distinct from the survived dwarf galaxies. The mergers debris have abundances expected for stars originating from dwarfs that had their star formation activity quenched at early times. Accreted stellar haloes, including individual debris, reveal abundance gradients in the ELz, where the most metal-rich stars have formed in the inner parts of the disrupted systems before the merger and mainly contribute to the central regions of the hosts. Therefore, we suggest that abundance measurements in the inner MW will allow constraining better the parameters of building blocks of the MW stellar halo. The MDFs of the individual debris show several peaks and the majority of debris have lower metallicity than the in-situ stars for $Lz > 0$, while non-rotating and retrograde accreted stars are similar to the in-situ. Prograde accreted stars show a prominent knee in the [Fe/H]-[Mg/Fe] plane while the retrograde stars typically deposit to a high-[Mg/Fe] sequence. We found that the metal-poor stars ([Fe/H]< -1) of the HESTIA galaxies exhibit between zero to 80 km/s net rotation which is consistent with the

Aurora population. At higher metallicities, we detect a sharp transition (spin-up) from the turbulent phase to a disk-like rotation. Mergers debris are similar in the [Fe/H]-[Mg/Fe] plane. However, combining a set of abundances allows to capture chemical patterns corresponding to different debris, which are the most prominent as a function of stellar age.

4.7 Structure of the Galaxy and Local Group

Ultra-diffuse galaxies (UDGs) are attractive candidates to probe cosmological models and test theories of galaxy formation at low masses; however, they are difficult to detect because of their low surface brightness. In the Local Group (LG) a handful of UDGs have been found to date, most of which are satellites of the Milky Way and M31, and only two are isolated galaxies. It is unclear whether so few UDGs are expected. Newton et al. (2022a) address this by studying the population of UDGs formed in hydrodynamic constrained simulations of the LG from the HESTIA suite. For a LG with mass MLG($< 2.5h^{-1}$ Mpc)$= 8 \times 10^{12} M_{\odot}$ (68 per cent confidence) are detectable in the footprint of the Sloan Digital Sky Survey (SDSS). Accounting for survey incompleteness, we find that up to 82, 90, and 100 per cent of all UDGs in the LG field would be observable in a future all-sky survey with a depth similar to the SDSS, the Dark Energy Survey, or the Legacy Survey of Space and Time, respectively. Our results suggest that there is a population of UDGs in the LG awaiting discovery.

Biaus et al. (2022) investigate the kinematic properties of gas and galaxies in the Local Group (LG) using high-resolution simulations performed by the HESTIA (High-resolution Environmental Simulations of The Immediate Area) collaboration. Our simulations include the correct cosmography surrounding LG-like regions consisting of two main spiral galaxies of $\approx 10^{12} M_{\odot}$, their satellites and minor isolated galaxies, all sharing the same large-scale motion within a volume of a few Mpc. We characterize the gas and galaxy kinematics within the simulated LGs, from the perspective of the Sun, to compare with observed trends from recent HST/COS absorption-line observations and LG galaxy data. To analyse the velocity pattern of LG gas and galaxies seen in the observational data, we build sky maps from the local standard of rest, and the Galactic and LG barycentre frames. Our findings show that the establishment of a radial velocity dipole at low/high latitudes, near the preferred barycentre direction, is a natural outcome of simulation kinematics for material outside the Milky Way virial radius after removing Galaxy rotation when the two main LG galaxies are approaching. Our results favour a scenario where gas and galaxies stream towards the LG barycentre producing a velocity dipole resembling observations. While our study shows in a qualitative way the global matter kinematics in the LG as part of its ongoing assembly, quantitative estimates of gas-flow rates and physical conditions of the LG gas have to await a more detailed modelling of the ionization conditions, which will be presented in a follow-up paper.

Dupuy et al. (2022): How the cosmic web feeds haloes, and fuels galaxy formation is an open question with wide implications. This study explores the mass assembly in the Local Group (LG) within the context of the local cosmography by employing simulations whose initial conditions have been constrained to reproduce the local environment. The goal of this study is to inspect whether the direction of accretion of satellites on to the Milky Way and Andromeda galaxies is related to the cosmic web. The analysis considers the three high-resolution simulations available in the HESTIA simulation suite, as well as the derived velocity shear and tidal tensors. We notice two eras in the LG accretion history, delimited by an epoch around $z \sim 0.7$. We also find that satellites can travel up to $\approx 4\ h^{-1}$ Mpc, relative to their parent halo before crossing its viral radius R200. Finally, we observe a strong alignment of the infall direction with the axis of slowest collapse of both tidal and shear tensors, implying satellites of the LG originated from one particular region of the cosmic web and were channeled towards

us via the process of accretion.This alignment is dominated by the satellites that enter during the early infall era, i.e. $z > 0.7$.

Newton et al. (2022b): The Local Group is a unique environment in which to study the astrophysics of galaxy formation. The proximity of the Milky Way and M31 enhances the frequency of interactions of the low-mass halo population with more massive dark matter haloes, which increases their concentrations and strips them of gas and other material. Some low-mass haloes pass through the haloes of the Milky Way or M31 and are either ejected into the field or exchanged between the two primary hosts. We use high resolution gas-dynamical simulations to describe a new class of field haloes that passed through the haloes of both the Milky Way and M31 at early times and are almost twice as concentrated as field haloes that do not interact with the primary pair. These 'Hermeian' haloes are distributed anisotropically at larger distances from the Local Group barycentre than the primary haloes and appear to cluster along the line connecting the Milky Way and M31. Hermeian haloes facilitate the exchange of dark matter, gas, and stars between the Milky Way and M31 and can enhance the star formation rates of the gas in the primary haloes during their interactions with them. We also show that some Hermeian haloes can host galaxies that, because they are embedded in haloes that are more concentrated than regular field haloes, are promising targets for indirect dark matter searches beyond the Milky Way virial radius and can produce signals that are competitive with those of some dwarf galaxies. Hermeian galaxies in the Local Group should be detectable by forthcoming wide-field imaging surveys.

Kalberla et al. (2022) used HI4PI data to analyze velocity and density fluctuations in the interstellar medium (ISM). They applied the Yuen et al. (2021) velocity decomposition algorithm (VDA) for separating such fluctuations in the position-position-velocity (PPV) space. In the first version of this manuscript they came to the conclusion that velocity and density fields are statistically correlated. Yuen et al. (2021) tried to reproduce these results and pointed to a likely mistake in the VDA expression that was used. We confirm that there was such a software problem. The statement that VDA derived density and velocity fields from HI4PI are anti-correlated needs to be withdrawn. Correct is that these density and velocity fields are uncorrelated. In turn major parts of the conclusions in the first version of this manuscript, based on an erroneous correlation, are invalid. The submission to A&A was withdrawn on 24 February 2022.

4.8 High-energy astrophysics

Albert et al. (2022) report on the $\gamma-$ray properties of the 2018 Galactic nova V392 Per, spanning photon energies $\approx 0.1GeV-100$ TeV by combining observations from the Fermi Gamma-ray Space Telescope and the HAWC Observatory. As one of the most rapidly evolving γ-ray signals yet observed for a nova, GeV $\gamma-$rays with a power-law spectrum with an index $\Gamma = 2.0 \pm 0.1$ were detected over 8 days following V392 Per's optical maximum. HAWC observations constrain the TeV $\gamma-$ray signal during this time and also before and after. We observe no statistically significant evidence of TeV $\gamma-$ray emission from V392 Per, but present flux limits. Tests disfavor the extension of the Fermi Large Area Telescope spectrum to energies above 5 TeV by 2 standard deviations (95%) or more. We fit V392 Per's GeV $\gamma-$rays with hadronic acceleration models, incorporating optical observations, and compare the calculations with HAWC limits.

Diesing et al. (2022): In August of 2021, Fermi-LAT, H.E.S.S., and MAGIC detected GeV and TeV $\gamma-$ray emission from an outburst of recurrent nova RS Ophiuchi. This detection represents the first very high energy $\gamma-$rays observed from a nova, and opens a new window to study particle acceleration. Both H.E.S.S. and MAGIC described the observed $\gamma-$rays as

arising from a single, external shock. In this paper, we perform detailed, multi-zone modeling of RS Ophiuchi's 2021 outburst including a self-consistent prescription for particle acceleration and magnetic field amplification. We demonstrate that, contrary to previous work, a single shock cannot simultaneously explain RS Ophiuchi's GeV and TeV emission, particularly the spectral shape and distinct light curve peaks. Instead, we put forward a model involving multiple shocks that reproduces the observed $\gamma-$ray spectrum and temporal evolution. The simultaneous appearance of multiple distinct velocity components in the nova optical spectrum over the first several days of the outburst supports the presence of distinct shocks, which may arise either from the strong latitudinal dependence of the density of the external circumbinary medium (e.g., in the binary equatorial plane versus the poles) or due to internal collisions within the white dwarf ejecta (as powers the $\gamma-$ray emission in classical novae).

Sokolovsky et al. (2022): Peaking at 3.7 mag on 2020 July 11, YZ Ret was the second-brightest nova of the decade. The nova's moderate proximity (2.7 kpc, from Gaia) provided an opportunity to explore its multiwavelength properties in great detail. Here, we report on YZ Ret as part of a long-term project to identify the physical mechanisms responsible for high-energy emission in classical novae. We use simultaneous Fermi/LAT and NuSTAR observations complemented by XMM-Newton X-ray grating spectroscopy to probe the physical parameters of the shocked ejecta and the nova-hosting white dwarf. The XMM-Newton observations revealed a supersoft X-ray emission which is dominated by emission lines of C V, C VI, N VI, N VII, and O VIII rather than a blackbody-like continuum, suggesting CO-composition of the white dwarf in a high-inclination binary system. Fermi/LAT-detected YZ Ret for 15 d with the $\gamma-$ray spectrum best described by a power law with an exponential cut-off at 1.9 ± 0.6 GeV. In stark contrast with theoretical predictions and in keeping with previous NuSTAR observations of Fermi-detected classical novae (V5855 Sgr and V906 Car), the $3.5 - 78$-keV X-ray emission is found to be two orders of magnitude fainter than the GeV emission. The X-ray emission observed by NuSTAR is consistent with a single-temperature thermal plasma model. We do not detect a non-thermal tail of the GeV emission expected to extend down to the NuSTAR band. NuSTAR observations continue to challenge theories of high-energy emission from shocks in novae.

Dabhade et al. (2022): Giant radio sources (GRSs) defined to be > 0.7 Mpc are the largest single objects in the Universe and can be associated with both galaxies (GRGs) and quasars (GRQs). They are important for understanding the evolution of radio galaxies and quasars whose sizes range from pc to Mpc scales and are also valuable probes of their environment. These radio-loud active galactic nuclei (RLAGN) interact with the interstellar medium of the host galaxy on small scales and the large-scale intracluster or intergalactic medium for the GRSs. With several new and sensitive surveys over the last few years, the number of known GRSs has increased many fold which has led a resurgence of interest in the field. This review article summarises our current understanding of these sources based on nearly five decades of research, and discusses the importance of the Square Kilometer Array (SKA) in addressing some of the outstanding questions.

Mahato et al. (2022): The GRQ catalogue is the compendium of all the GRQs reported in the literature and our new GRQ sample. It consists of 265 sources, out of which 121 are from the GRG catalogue in SAGAN.I (Dabhade et al. 2020b), 134 are from KJ21, and 10 are the new GRQs reported in this paper. In order to compare the properties of GRQs with SRQs, one needs to create a robust SRQ catalogue (size < 700kpc). Hence, we compiled a sample of SRQs from the catalogue of Kimball et al. (2011, Cat. J/AJ/141/182)

Pandge et al. (2022) present original Giant Metrewave Radio Telescope (GMRT) radio observations of the galaxy cluster Abell 725, at a redshift (z) of 0.09, along with other archival

observations. Our GMRT maps reveal two steep-spectrum diffuse filaments in the cluster, along with a previously reported arc-like structure, and a wide-angle-tail (WAT) radio source associated with the brightest cluster galaxy (BCG) at the periphery of the cluster. The bent morphology of the WAT indicates that its jets have been swept back by the dynamic pressure resulting from the motion of the BCG through the surrounding intracluster medium. The BCG associated with the WAT hosts a black hole whose mass we estimate to be $1.4 \pm 0.4 \times 10^9\ M_\odot$. We observe a 2 arcmin (195 kpc in projection) offset between the BCG and the X-ray centroid of the galaxy cluster, which, along with other dynamic features, indicates the cluster's early stage of evolution. The WAT radio galaxy, the arc, and the filaments have spectral indices $\alpha 240612 = -0.46 \pm 0.15$, -0.8 ± 0.3, and (-1.13 ± 0.48, -1.40 ± 0.50), respectively. The WAT and the arc are connected structures, while the filaments are detached from them, but are found to be along the trail of the WAT. Based on the morphology of the components, and the progressive steepening of the components from the core of the WAT to the filaments, we propose that this system is a radio galaxy with trailing antique filaments.

4.9 Study of stellar evolution

Liimets et al. (2022): Context. V838 Monocerotis is a peculiar binary that underwent an immense stellar explosion in 2002, leaving behind an expanding cool supergiant and a hot B3V companion. Five years after the outburst, the B3V companion disappeared from view, and so far did not recover. Aims. We investigate the changes in the light curve and spectral features Methods. A monitoring campaign has been performed during the past 13 years with the Nordic Optical Telescope to obtain optical photometric and spectroscopic data. The data sets are used to analyse the temporal evolution of the spectral features and the spectral energy distribution, and to characterize the object. Results. Our photometric data show a steady brightening in all bands during the past 13 years, which is particularly prominent in the blue. This rise is also reflected in the spectra, showing a gradual relative increase in the continuum flux at shorter wavelengths. In addition, a slow brightening of the Ha emission line starting in 2015 was detected. These changes might imply that the B3V companion is slowly reappearing. During the same time interval, our analysis reveals a considerable change in the observed colours of the object along with a steady decrease in the strength and width of molecular absorption bands in our low-resolution spectra. These changes suggest a rising temperature of the cool supergiant along with a weakening of its wind, most likely combined with a slow recovery of the secondary due to the evaporation of the dust and accretion of the material from the shell in which the hot companion is embedded. From our medium-resolution spectra, we find that the heliocentric radial velocity of the atomic absorption line of TiI 6556.06 A has been stable for more than a decade. We propose that TiI lines are tracing the velocity of the red supergiant in V838 Mon, and not representing the infalling matter as previously stated.

Nesci et al. (2022b): Light curves for 165 Maffei's variables were found in the OGLE GVS database, with a typical sampling for each star of about 100 points over a 5-year time span, comparable to that of Maffei's light curves. The photometric errors were usually smaller than 0.01mag. A few known eclipsing variables were excluded, as well as a few very poorly sampled stars, giving a final sample of 150 stars.

Nesci et al. (2022a) analyzed the light curves of 165 AGB variables, mostly Miras, in the sky area centered between M16 and M17 ($l = 16, b = 0$), using the OGLE GVS database in the Ic band. Comparison with the published light curves, derived about 50 years earlier by P. Maffei using Kodak I-N photographic plates, allowed us to find no significant period changes in any star. Remarkably, a few stars of the sample appear to have substantially changed their average luminosity, the most striking case being KZ Ser. We provide a better identification for

three stars: IX Ser, NSV 10522, and NSV 10326, all of them being Miras. We classify the light curves of 6 stars, discovered but not classified by Maffei, (GL Ser, NSV 10271, NSV 10326, NSV 10522, NSV 10677, and NSV 10772) five of them being new Miras, and confirm the R CrB nature of V391 Sct. The magnitude scale used by Maffei is compared to the modern Ic one.

5 List of collaborators

Elmo Tempel (PhD, Prof., head of Department of Physics of Galaxies and Cosmology);
Jaan Einasto (Prof. DSc, science consultant);
Maret Einasto, DSc, associate professor);
Urmas Haud (DSc, associate professor);
Heidi Lietzen (PhD, associate professor);
Jukka Nevalainen (PhD, associate professor);
Antti Tamm (PhD, associate professor);
Peeter Tenjes (DSc, associate professor);
Indrek Vurm (DSc, associate professor);
Rain Kipper (PhD, scientist);
Jaan Laur (PhD, scientist);
Juhan Liivamägi (PhD, scientist);
Taavi Tuvikene (PhD, scientist);
Teet Kuutma (PhD, junior scientist);
Maria Jose Benito (PhD, visiting scientist);
Shishir Sankhyayan PhD, (visiting scientist);
Moorits Mihkel Muru (MSc, junior scientist);
Toni Tuominen (MSc, junior scientist);
Aikaterini Niovi Triantafyllaki (MSc, visiting scientist);
Jad-Alexandru Mansour (MSc, visiting scientist);
Mousumi Mahato (MSc, visiting scientist).

References

Albert, A., Alfaro, R., Alvarez, C., Arteaga-Velázquez, J. C., Rojas, D. A., Solares, H. A. A., Babu, R., Belmont-Moreno, E., Blochwitz, C., Caballero-Mora, K. S., Capistrán, T., Carramiñana, A., Casanova, S., et al. 2022, *γ-Ray Emission from Classical Nova V392 Per: Measurements from Fermi and HAWC*, ApJ, 940, 141

Bazarov, A., Benito, M., Hütsi, G., Kipper, R., Pata, J., & Põder, S. 2022, *Sensitivity estimation for dark matter subhalos in synthetic Gaia DR2 using deep learning*, Astronomy and Computing, 41, 100667

Biaus, L., Nuza, S. E., Richter, P., Sparre, M., Scannapieco, C., Damle, M., Sorce, J. G., Grand, R. J. J., Tempel, E., Libeskind, N. I., & Hani, M. H. 2022, *Kinematics of the Local Group gas and galaxies in the HESTIA simulations*, MNRAS, 517, 6170

Dabhade, P., Saikia, D. J., & Mahato, M. 2022, *Decoding the giant extragalactic radio sources*, arXiv e-prints, arXiv:2208.02130

Damle, M., Sparre, M., Richter, P., Hani, M. H., Nuza, S. E., Pfrommer, C., Grand, R. J. J., Hoffman, Y., Libeskind, N., Sorce, J. G., Steinmetz, M., Tempel, E., Vogelsberger, M., & Wang, P. 2022, *Cold and hot gas distribution around the Milky-Way - M31 system in the HESTIA simulations*, MNRAS, 512, 3717

de Jong, R. S., Bellido-Tirado, O., Brynnel, J. G., Ezzati Amini, A., Frey, S., Füßlein, C., Gäbler, M., Giannone, D., Johl, D., Kuba, S., Lemke, U., Micheva, G., Saviauk, A., et al. 2022, *4MOST: the 4-metre multi-object spectroscopic telescope project in the assembly, integration, and test phase*, in Society of Photo-Optical Instrumentation Engineers (SPIE) Conference Series, Vol. 12184, Ground-based and Airborne Instrumentation for Astronomy IX, ed. C. J. Evans, J. J. Bryant, & K. Motohara, 1218414

Diesing, R., Metzger, B. D., Aydi, E., Chomiuk, L., Vurm, I., Gupta, S., & Caprioli, D. 2022, *Evidence for multiple shocks from the γ-ray emission of RS Ophiuchi*, arXiv e-prints, arXiv:2211.02059

Dupuy, A., Libeskind, N. I., Hoffman, Y., Courtois, H. M., Gottlöber, S., Grand, R. J. J., Knebe, A., Sorce, J. G., Tempel, E., Tully, R. B., Vogelsberger, M., & Wang, P. 2022, *Anisotropic satellite accretion on to the Local Group with HESTIA*, MNRAS, 516, 4576

Einasto, J., Liivamägi, L. J., & Einasto, M. 2023, *The time evolution of bias*, MNRAS, 518, 2164

Einasto, M., Kipper, R., Tenjes, P., Einasto, J., Tempel, E., & Liivamägi, L. J. 2022a, *Death at watersheds: Galaxy quenching in low-density environments*, A&A, 668, A69

Einasto, M., Tenjes, P., Gramann, M., Lietzen, H., Kipper, R., Liivamägi, L. J., Tempel, E., Sankhyayan, S., & Einasto, J. 2022b, *The evolution of high-density cores of the BOSS Great Wall superclusters*, A&A, 666, A52

Heinämäki, P., Teerikorpi, P., Douspis, M., Nurmi, P., Einasto, M., Gramann, M., Nevalainen, J., & Saar, E. 2022, *Quasi-spherical superclusters*, A&A, 668, A37

Holt, P., Tuominen, T., Nevalainen, J., Bonamente, M., Kuutma, T., Heinämäki, P., & Tempel, E. 2022, *The scaling relation between galaxy luminosity and WHIM density from EAGLE simulations with application to SDSS data*, MNRAS, 513, 3387

Hütsi, G., Raidal, M., Urrutia, J., Vaskonen, V., & Veermäe, H. 2022, *Did JWST observe imprints of axion miniclusters or primordial black holes?*, arXiv e-prints, arXiv:2211.02651

Kalberla, P. M. W., Kerp, J., & Haud, U. 2022, *Correlations between turbulent velocity and density fields in the local interstellar medium*, arXiv e-prints, arXiv:2202.01610

Khoperskov, S., Minchev, I., Libeskind, N., Belokurov, V., Steinmetz, M., Gomez, F. A., Grand, R. J. J., Knebe, A., Sorce, J. G., Sparre, M., Tempel, E., & Vogelsberger, M. 2022a, *The stellar halo in Local Group Hestia simulations III. Chemical abundance relations for accreted and in-situ stars*, arXiv e-prints, arXiv:2206.05491

Khoperskov, S., Minchev, I., Libeskind, N., Haywood, M., Di Matteo, P., Belokurov, V., Steinmetz, M., Gomez, F. A., Grand, R. J. J., Knebe, A., Sorce, J. G., Sparre, M., Tempel, E., & Vogelsberger, M. 2022b, *The stellar halo in Local Group Hestia simulations I. The in-situ component and the effect of mergers*, arXiv e-prints, arXiv:2206.04521

Khoperskov, S., Minchev, I., Libeskind, N., Haywood, M., Di Matteo, P., Belokurov, V., Steinmetz, M., Gomez, F. A., Grand, R. J. J., Knebe, A., Sorce, J. G., Sparre, M., Tempel, E., & Vogelsberger, M. 2022c, *The stellar halo in Local Group Hestia simulations II. The accreted component*, arXiv e-prints, arXiv:2206.04522

Laur, J., Tempel, E., Tamm, A., Kipper, R., Liivamägi, L. J., Hernán-Caballero, A., Muru, M. M., Chaves-Montero, J., Díaz-García, L. A., Turner, S., Tuvikene, T., Queiroz, C., Bom, C. R., et al. 2022, *TOPz: Photometric redshifts for J-PAS*, A&A, 668, A8

Liimets, T., Kolka, I., Kraus, M., Eenmäe, T., Tuvikene, T., Augusteijn, T., Antunes Amaral, L., Djupvik, A. A., Telting, J. H., Deshev, B., Kankare, E., Kankare, J., Lindberg, J. E., et al. 2022, *V838 Mon: A slow waking up of Sleeping Beauty?*, arXiv e-prints, arXiv:2211.06629

Mahato, M., Dabhade, P., Saikia, D. J., Combes, F., Bagchi, J., Ho, L. C., & Raychaudhury, S. 2022, *VizieR Online Data Catalog: SAGAN III. New insights into giant radio quasars (Mahato+, 2022)*, VizieR Online Data Catalog, J/A+A/660/A59

Nesci, R., Soszynski, I., & Tuvikene, T. 2022a, *Period Changes of Mira Variables in the M16 - M17 Region*, Open European Journal on Variable Stars, 230, 1

Nesci, R., Soszynski, I., & Tuvikene, T. 2022b, *VizieR Online Data Catalog: Mira variables period changes in M16-M17 Region (Nesci+, 2022)*, VizieR Online Data Catalog (other), 0430, J/other/OEJV/230

Newton, O., Di Cintio, A., Cardona-Barrero, S., Libeskind, N. I., Hoffman, Y., Knebe, A., Sorce, J., Steinmetz, M., & Tempel, E. 2022a, *The undiscovered ultra-diffuse galaxies of the Local Group*, arXiv e-prints, arXiv:2212.05066

Newton, O., Libeskind, N. I., Knebe, A., Sánchez-Conde, M. A., Sorce, J. G., Pilipenko, S., Steinmetz, M., Pakmor, R., Tempel, E., Hoffman, Y., & Vogelsberger, M. 2022b, *Hermeian haloes: Field haloes that interacted with both the Milky Way and M31*, MNRAS, 514, 3612

Pandge, M. B., Kale, R., Dabhade, P., Mahato, M., & Raychaudhury, S. 2022, *Giant Metrewave Radio Telescope unveils steep-spectrum antique filaments in the galaxy cluster Abell 725*, MNRAS, 509, 1837

Parekh, V., Kincaid, R., Thorat, K., Hugo, B., Sankhyayan, S., Kale, R., Oozeer, N., Smirnov, O., Heywood, I., Makhathini, S., & van der Heyden, K. 2022, *MOSS I: Double radio relics in the Saraswati supercluster*, MNRAS, 509, 3086

Sokolovsky, K. V., Li, K.-L., Lopes de Oliveira, R., Ness, J.-U., Mukai, K., Chomiuk, L., Aydi, E., Steinberg, E., Vurm, I., Metzger, B. D., Babul, A.-N., Kawash, A., Linford, J. D., et al. 2022, *The first nova eruption in a novalike variable: YZ Ret as seen in X-rays and γ-rays*, MNRAS, 514, 2239

December 20, 2022